Effect of Sampling Temperature on the Properties of Inorganic Particulate Matter Collected from Biomass Combustion in a Drop-Tube Furnace

ARTICLE *in* ENERGY & FUELS · AUGUST 2010

Impact Factor: 2.79 · DOI: 10.1021/ef100701r

2 AUTHORS:

Xiangpeng Gao
Curtin University
30 PUBLICATIONS **319** CITATIONS
SEE PROFILE

Hongwei Wu
Yale University
91 PUBLICATIONS **2,402** CITATIONS
SEE PROFILE

Energy Fuels **2010,** *24,* 4571–4580 · DOI:10.1021/ef100701r
Published on Web 07/28/2010

energy&fuels
article

Effect of Sampling Temperature on the Properties of Inorganic Particulate Matter Collected from Biomass Combustion in a Drop-Tube Furnace

Xiangpeng Gao and Hongwei Wu*

Curtin Centre for Advanced Energy Science and Engineering, Department of Chemical Engineering, Curtin University of Technology, GPO Box U1987, Perth WA 6845, Australia

Received June 6, 2010. Revised Manuscript Received July 12, 2010

Sampling temperature is found to significantly influence the properties of PM_{10} (particulate matter with an aerodynamic diameter less than 10.0 μm) collected from the combustion of pulverized biomass (75−150 μm) in a laboratory-scale drop-tube furnace system at 1300 °C. Although the $PM_{1.0}$ yield remains constant, the mass of $PM_{1.0}$ shifts to a larger size at a lower sampling temperature, apparently due to particulate coagulation. $PM_{1.0}$ dominantly contains Na, K, and Cl, and the mass size distribution of these elements also shifts to a larger size as the sampling temperature decreases. However, $PM_{1.0-10}$ dominantly consists of Ca, Mg, and S. Increasing sampling temperature reduces PM loss due to gravitational settling deposition, leading to an increase in the $PM_{1.0-10}$ yield. The mass of Mg and Ca in $PM_{1.0-10}$ also increases with increasing sampling temperature and reaches constant values at sampling temperatures close to the flue gas temperature (115 °C). The sampling temperatures at which drastic shifts in particle size distribution and elemental mass size distribution of PM_{10} take place correlate well with the SO_3 dew points of the flue gas. The results in this study suggest that the sampling temperature of PM should be above the flue gas acid dew point to prevent the condensation of acid gas and, furthermore, be kept close to or same as the flue gas temperature in order to suppress particulate coagulation and gravitational settling deposition.

1. Introduction

Mallee biomass is a key second-generation bioenergy feedstock for the future sustainable development of rural and regional Australia.[1−3] Direct biomass combustion or cofiring of biomass and coal is matured technology for power generation from mallee biomass but may contribute significantly to particulate matter (PM) emission. Particularly, PM with an aerodynamic diameter less than 1.0 μm ($PM_{1.0}$), 2.5 μm ($PM_{2.5}$), and 10.0 μm (PM_{10}) are known to have significant adverse impact on both human health and the environment.[4−6] Therefore, a thorough understanding on PM properties and formation during biomass combustion is required for minimizing PM emissions from the combustion of biomass such as mallee.

Sampling of PM from solid fuel (coal or biomass) combustion systems typically employs a combination of cyclone and low pressure impactor (LPI). As summarized in Table 1, a review on the sampling methods used in some previous studies[7−22] shows that those studies used significantly different sampling conditions. Dilution is for both quenching flue gas and preventing particle overloading in sampling instruments.[23,24] It is clear that the previous studies employed very different dilution conditions. Various sampling temperatures were also used in those studies, ranging from room temperature to 150 °C. As shown in Table 1, such information was not given in some of the studies. Obviously, there is no standard method for PM sampling. Although limited

*To whom correspondence should be addressed. E-mail: h.wu@curtin.edu.au. Telephone: +61-8-92667592. Fax: +61-8-92662681.

(1) Wu, H.; Fu, Q.; Giles, R.; Bartle, J. *Energy Fuels* **2008**, *22*, 190–198.
(2) Yu, Y.; Bartle, J.; Li, C. Z.; Wu, H. *Energy Fuels* **2009**, *23*, 3290–3299.
(3) Bartle, J. R.; Abadi, A. *Energy Fuels* **2010**, *24*, 2–9.
(4) Lind, T.; Valmari, T.; Kauppinen, E. I.; Sfiris, G.; Nilsson, K.; Maenhaut, W. *Environ. Sci. Technol.* **1999**, *33*, 496–502.
(5) Maynard, A. D.; Maynard, R. L. *Atmos. Environ.* **2002**, *36*, 5561–5567.
(6) WHO, Air quality guidelines: Global update 2005, World Health Organization, ISBN: 9289021926, 2007 Edition.
(7) Kauppinen, E. I.; Pakkanen, T. A. *Environ. Sci. Technol.* **1990**, *24*, 1811–1818.
(8) Valmari, T.; Lind, T. M.; Kauppinen, E. I.; Sfiris, G.; Nilsson, K.; Maenhaut, W. *Energy Fuels* **1999**, *13*, 379–389.
(9) Seames, W. S. *Fuel Process. Technol.* **2003**, *81*, 109–125.
(10) Johansson, L. S.; Leckner, B.; Gustavsson, L.; Cooper, D.; Tullin, C.; Potter, A. *Atmos. Environ.* **2004**, *38*, 4183–4195.
(11) Strand, M.; Bohgard, M.; Swietlicki, E.; Gharibi, A.; Sanati, M. *Aerosol Sci. Technol.* **2004**, *38*, 757–765.
(12) Buhre, B. J. P.; Hinkley, J. T.; Gupta, R. P.; Wall, T. F.; Nelson, P. F. *Fuel* **2005**, *84*, 1206–1214.
(13) Boman, C.; Nordin, A.; Westerholm, R.; Pettersson, E. *Biomass Bioenergy* **2005**, *29*, 258–268.
(14) Jimenez, S.; Ballester, J. *Proc. Combust. Inst.* **2005**, *30*, 2965–2972.
(15) Liu, X.; Xu, M.; Yao, H.; Yu, D.; Gao, X.; Cao, Q.; Cai, Y. *Energy Fuels* **2006**, *21*, 157–162.
(16) Takuwa, T.; Mkilaha, I. S. N.; Naruse, I. *Fuel* **2006**, *85*, 671–678.
(17) Linak, W. P.; Yoo, J.-I.; Wasson, S. J.; Zhu, W.; Wendt, J. O. L.; Huggins, F. E.; Chen, Y.; Shah, N.; Huffman, G. P.; Gilmour, M. I. *Proc. Combust. Inst.* **2007**, *31*, 1929–1937.
(18) Zhang, L.; Masui, M.; Mizukoshi, H.; Ninomiya, Y.; Koketsu, J.; Kanaoka, C. *Fuel* **2008**, *87*, 964–973.
(19) Bäfver, L. S.; Rönnbäck, M.; Leckner, B.; Claesson, F.; Tullin, C. *Fuel Process. Technol.* **2009**, *90*, 353–359.
(20) Wiinikka, H.; GrÖnberg, C.; Öhrman, O.; BostrÖm, D. *Energy Fuels* **2009**, *23*, 5367–5374.
(21) Ninomiya, Y.; Wang, Q.; Xu, S.; Mizuno, K.; Awaya, I. *Energy Fuels* **2009**, *23*, 3412–3417.
(22) Ninomiya, Y.; Wang, Q.; Xu, S.; Teramae, T.; Awaya, I. *Energy Fuels* **2010**, *24*, 199–204.
(23) Markowski, G. R.; Ensor, D. S.; Hooper, R. G.; Carr, R. C. *Environ. Sci. Technol.* **1980**, *14*, 1400–1402.
(24) Wehner, B.; Bond, T. C.; Birmili, W.; Heintzenberg, J.; Wiedensohler, A.; Charlson, R. J. *Environ. Sci. Technol.* **1999**, *33*, 3881–3886.

Table 1. Summary of PM Sampling Methods from Solid Fuels (Biomass or Coal) Combustion in Some Previous Studies

reference	study type	fuel	combustion system	sampling system	sampling temperature	dilution
Kauppinen et al.[7]	field study	bituminous coal	a pulverized coal boiler	BLPI[a]	112−123 °C	NA[h]
Valmari et al.[8]	field study	forest residue + willow	a circulating fluidized-bed boiler	cyclone + BLPI[a]	110−120 °C	dilution ratio 80:1
Seames[9]	lab-scale	bituminous + subbituminous coal	a downflow laboratory combustor	cyclone + BLPI[a]	NA[h]	dilution applied but dilution ratio not given
Johansson et al.[10]	field study	wood pellets + bark pellets + wood briquettes + wood logs	residential boilers	cyclone + ELPI[b] + DLPI[c]	room temperature	2 stage dilution but dilution ratio not given
Strand et al.[11]	field study	forest residue + peat	a circulating fluidized bed boiler	SMPS[d] + ELPI[b] + DLPI[c]	25 °C	dilution ratio 60:1
Buhre et al.[12]	lab-scale	bituminous coal	a drop-tube furnace	cyclone + CI[e]	room temperature	NA[h]
Boman et al.[13]	field-study	softwood pellets	a residential pellet stove	cyclone + DLPI[c]	45−75 °C	dilution ratio from 3:1 to 7:1
Jimenez and Ballester[14]	lab-scale	orujillo + coal + coke	a down-fired entrained flow reactor	cyclone + BLPI[a]	∼130 °C	NA[h]
Takuwa et al.[16]	lab-scale	coal	a drop tube furnace	LPI[f]	NA[h]	dilution ratio 10
Liu et al.[15]	lab-scale	bituminous coal	a drop-tube furnace	cyclone + DLPI[c]	NA[h]	NA[h]
Linak et al.[17]	lab-scale	pulverized coal	a down-fired lab-scale combustor + a drop tube furnace.	cyclone + BLPI[a] or MOUDI[g]	80 °C	dilution applied but dilution ratio not given
Zhang et al.[18]	field-study	sewage sludge	an incineration plant	LPI[f]	room temperature	dilution ratio 20:3
Bäfver et al.[19]	field study	oat grain	a combifire boiler	cyclone + DLPI[c] + ELPI[b]	105 °C	NA[h]
Wiinikka et al.[20]	lab-scale	straw pellets	a fixed bed reactor with a pellets burner	cyclone + DLPI[c]	>150 °C	NA[h]
Ninomiya et al.[21,22]	lab-scale	bituminous coals	a drop-tube furnace	cyclone + LPI[f]	NA[h]	dilution ratio 6

[a] BLPI: Berner-type Low Pressure Impactor. [b] ELPI: Electrical Low Pressure Impactor. [c] DLPI: Dekati Low Pressure Impactor. [d] SMPS: Scanning Mobility Particle Sizer. [e] CI: Cascade Impactor. [f] LPI: Low Pressure Impactor. [g] MOUDI: Micro-Orifice Uniform Deposition Impactor. [h] NA: relevant information not available in the publications.

attempts were made to study the effects of sampling methods (particularly dilution ratio) on PM properties, there is significant discrepancy in conclusions drawn in different studies.[13,25] Therefore, the validity is also questionable in comparing the experimental data in different studies.

Therefore, sampling conditions are clearly important considerations to ensure that the properties of PM collected are not distorted by the sampling process. The key objective of this study is to carry out a systematic investigation on the effect of sampling temperature on the properties of particulate matter generated from biomass combustion, while other conditions are kept unchanged. A mallee bark sample is combusted in a drop-tube furnace system under constant conditions to generate a constant stream of PM_{10}-containing flue gas (exit temperature: 115 °C). A proper method is then developed for sampling and characterizing the PM collected.

2. Experimental Section

2.1. Preparation of Malee Bark Sample. A biomass sample (mallee bark) was prepared by separating the bark component from the green mallee trees (*E.loxophleba lissophloia*), which were harvested from Narrogin, Western Australia. After being dried at 40 °C in a large lab oven, the bark sample was then cut, milled, and sieved into the size fraction of 75−150 μm. The prepared sample was stored in sealed double bags in a freezer under −4 °C. The fuel properties of the prepared mallee bark sample are summarized in Table 2.

2.2. Experimental Setup. As shown in Figure 1, the experimental system is composed of a constant PM generator and a PM sampling system. A lab-scale drop-tube furnace (DTF) was used as ash particle generator to produce a constant ash particle source from bark combustion. The DTF operates at 1 atm and a maximum temperature of 1600 °C under various atmospheres. It consists of a feeding system, main reactor, and a water-cooled quench probe. The feeding system is similar to the one used in a previous study[26] but modified for biomass fuels, including an entrained flow feeder, primary air, mass flow controller, and a water-cooled feeding probe. Fuel particles are entrained by primary air and fed into the reactor via the water-cooled feeding probe. The secondary air was introduced through the feeding probe to provide a laminar flow profile in the heated zone of the reactor. The main reactor is an electrically heated vertical mullite reaction tube (inner diameter of 54 mm, length of 1200 mm), with an isothermal zone of ∼600 mm. The water-cooled quench probe, using helium as quench medium (1 L/min), was designed not only for quick quenching and diluting the particle stream with high purity helium to minimize the interaction among particles but also for forcing the nucleation of vaporized materials. The furnace temperature was kept at 1300 °C. The total combustion air flow rate (primary air and secondary air) was 5.6 L/min. The residence time of bark particles in the isothermal zone was estimated as ∼1.7s.

This study considers two different steams of constant PM_{10}-containing flue gas with different particle mass concentrations and acid gas (mainly SO_3 and HCl) concentrations at the outlet of water-cooled quench probe (termed as point A; see Figure 1).

(25) Lipsky, E.; Stanier, C. O.; Pandis, S. N.; Robinson, A. L. *Energy Fuels* **2002**, *16*, 302–310.

(26) Quyn, D. M.; Wu, H.; Li, C. Z. *Fuel* **2002**, *81*, 143–149.

Table 2. Properties of *E. loxophleba lissophloia* Mallee Bark Used in This Study

	proximate analysis, % db			ultimate analysis, % daf					
moisture, % after pre-dried	ash	VM[a]	FC[b]	C	H	N	S	Cl	O[c]
4.9	4.9	68.1	27.0	52.0	5.78	0.41	0.04	0.18	41.59

[a] Volatile matter. [b] Fixed carbon. [c] By difference.

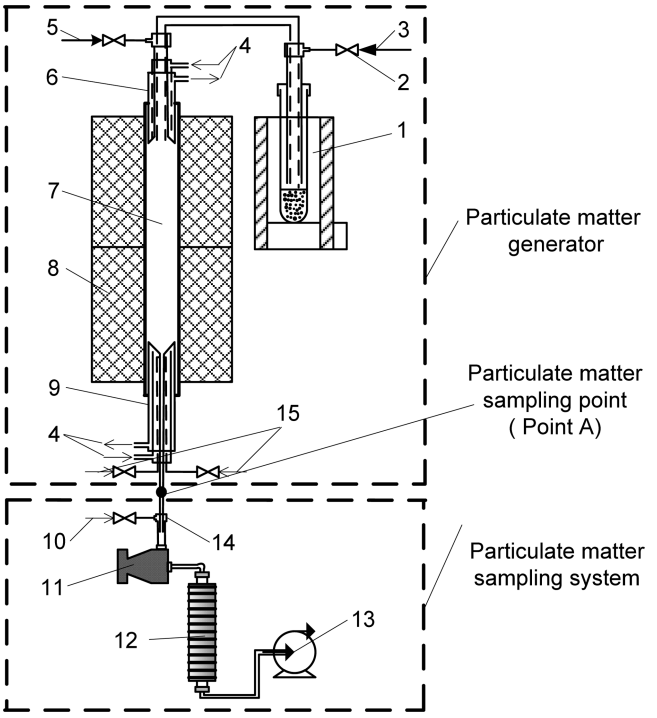

Figure 1. Schematic diagram of experimental setup: (1) feeder, (2) mass flow controller, (3) primary air, (4) cooling water, (5) secondary air, (6) water-cooled feeding probe, (7) mullite reaction tube, (8) two heating-zone furnace, (9) water-cooled quench probe, (10) makeup and dilution air, (11) cyclone, (12) Dekati low pressure impactor, (13) vacuum pump, (14) diluter, and (15) quench helium.

This was achieved using two fuel feeding rates (0.1 and 0.3 g/min, denoted as "Case-0.1" and "Case-0.3" hereafter) with all other experimental conditions kept unchanged. Preliminary tests were carried out to adjust the flue gas temperature at the exit of the quench probe (point A; see Figure 1) as 115 °C, via adjusting probe position and the flow rates of quench helium and cooling water. In all subsequent experiments, these parameters were then maintained unchanged. All experiments were also carefully designed and carried out under conditions with substantial excessive air. The values of lambda (λ, expressed as the ratio of actual air−fuel ratio to stoichiometric air−fuel ratio) in Case-0.1 and Case-0.3 are ~13 and ~4.3, respectively. The high furnace temperature (1300 °C), fine biomass particle size (75−150 μm), and substantial excessive air facilitates operation conditions which achieve complete combustion. Indeed, the total organic carbon (TOC) analysis of the extracts of PM samples shows that little organic carbon is present in the PM samples collected from all experiments.

The PM sampling system consists of a diluter, a Dekati cyclone (Model SAC-65), a Dekati low pressure impactor (DLPI) with backup filter, and a vacuum pump (Leybold Sogevac SV25). The DLPI used here is composed of 13 collection stages, calibrated by the manufacturer. The inlet and outlet pressure of the DLPI was controlled at 1013.3 and 100 mbar, respectively. The bottom stage of DLPI acts as a sonic orifice to control the flow rate at nominal value (~10 L/min). Because the total gas streamflow rate (including primary air, secondary air, and quench helium) was lower than 10 L/min, a small steam (~3.4 L/min) of instrument grade air was introduced through the diluter as makeup and dilution air (with a dilution ratio of 1.5). Because the feeding rate of biomass is very low, the PM_{10} concentration in the flue gas at the furnace exit is low so that no further dilution was carried out during sampling. Therefore, the overall dilution ratio is constant in all experiments.

2.3. Sampling of Particulate Matter. The PM_{10}-containing flue gas was first separated by the cyclone to remove the coarse ash particles (aerodynamic diameter > 10 μm), then directed to the DLPI for size-segregated collection (0.0275−10 μm), and the ultrafine particles (< 0.0275 μm) were collected by the backup filter. As suggested by the manufacturer (Dekati), the cyclone was placed horizontally for all the experiments to minimize the effect of the tube bend in the sampling line (see Figure 1). Aluminum foils and polycarbonate filters were used as collection substrates for the mass concentration and chemical analysis, respectively. The collection substrates were greased by Apiezon-H vacuum grease to prevent particle bounce and were pretreated at 115 °C for 12 h to avoid mass losses (if any) during sampling. To study the effect of sampling temperature on PM collection, the sampling system (including diluter, cyclone, DLPI, and the stainless steel sampling lines) was adjusted at various temperatures (25−115 °C) via external electrical heating. At different sampling temperatures, the actual cutoff aerodynamic diameters of cyclone and DLPI under various sampling temperatures were different with the calibration values and were properly corrected by the calculation program provided by the manufacturer (Dekati). After the experiment, the collection substrates were carefully disassembled and put in a desiccator. The collection substrates were analyzed gravimetrically with a 0.001 mg microbalance (Mettler MX5). The relative standard errors of PM mass size distribution are ±4%. The ash particles collected by the cyclone and deposited in the sampling tubing were washed by acetone and weighed after the evaporation of acetone.

2.4. Sample Analysis. The contents of alkali and alkaline earth metallic species (AAEM species, mainly Na, K, Mg, and Ca) in the bark sample were determined via a procedure[27] that was developed on the basis of a method used previously for brown coals.[28] Briefly, 20−30 mg of bark sample was put in a Pt crucible, and then, it was ashed in air following a specially designed heating program (from room temperature to 600 °C) to ensure no loss of these species during ashing. The ash sample together with the Pt crucible was then put in a Teflon vial for acid digestion with a mixture of HNO_3/HF (1:1) solution at 120 °C for 12 h. After the evaporation of excessive acids on a hot plate, the digested ash was dissolved in 20 mM methanesulfonic acid (MSA) solution. The AAEM species in the solution was quantified using a Dionex ICS-3000 ion chromatography with a CS12A column and 20 mM MSA solution as eluent. Other inorganic species (Al, Ba, Fe, P, Si, Sr, and Ti) in the raw bark sample were analyzed by an inductively coupled plasma-atomic emission spectroscopy (ICP-AES). The detailed analysis procedure can be found elsewhere.[27] Table 3 shows the contents of inorganic species in raw bark sample. As shown in Tables 2 and 3, the bark sample has high contents of AAEM species

(27) Yip, K.; Tian, F.; Hayashi, J.; Wu, H. *Energy Fuels* **2010**, *24*, 173–181.

(28) Li, C. Z.; Sathe, C.; Kershaw, J. R.; Pang, Y. *Fuel* **2000**, *79*, 427–438.

Table 3. Contents (wt % Dry Basis) of Inorganic Species in the Mallee Bark Sample

Na[a]	K[a]	Mg[a]	Ca[a]	Si[b]	Al[b]	Ba[b]	Fe[b]	P[b]	Sr[b]	Ti[b]
0.2729	0.1353	0.0992	2.4717	0.0478	0.0093	0.0062	0.0065	0.0289	0.0317	0.0004

[a] Analyzed by IC. [b] Analyzed by ICP-AES.

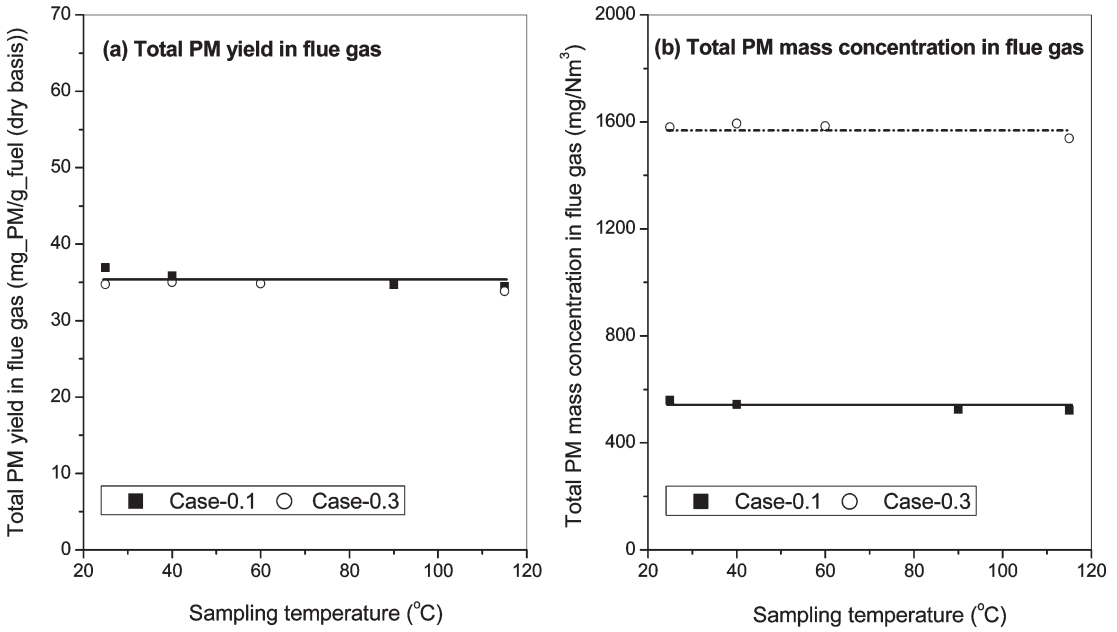

Figure 2. Total PM yield and mass concentration at point A: (a) total PM yield in flue gas and (b) total PM mass concentration in flue gas.

(~96% of the total inorganic species in bark) and Cl, while the contents of Si and Al are very low (< 2% of the total inorganic species in bark). Such unique features of the bark sample provide a simple system for this study. Therefore, the chemical composition analysis of the particulate matter in the present study focused on AAEM species, S, and Cl.

For the PM samples collected by the DLPI, two batches of experiments under the identical experimental conditions were carried out: one for AAEM species analysis and the other for S and Cl analysis. One batch of the PM-loaded polycarbonate filters were placed in Teflon vials for acid digestion and then analyzed by ion chromatography for AAEM species following the same procedure described above. The other batch of PM-loaded polycarbonate filters was dissolved into Milli-Q water for sufficiently long time (24 h) until all of the S and Cl were dissolved. The S and Cl in the solution were quantified using a Dionex ICS-1000 ion chromatography with an AS14 column and 3.5 mM $NaCO_3$/1.0 mM $NaHCO_3$ solution as eluent. The relative standard errors of the elemental mass size distribution for Na, K, Cl, and S are ±5% while those of Mg and Ca are ±6% and ±8%, respectively.

3. Results and Discussion

3.1. Measured PM Yields and Mass Concentrations in Flue Gas. At a given biomass feeding rate (0.1 or 0.3 g/min), the total PM yield (normalized to the amount of biomass combusted) and mass concentration are constant in all experiments at various sampling temperatures (see Figure 2). The PM mass concentration at a 0.3 g/min biomass feeding rate is about 3 times as that at the 0.1 g/min biomass feeding rate, while the total PM yield normalized to the amount of biomass combusted remains unchanged. This is expected as the configuration of the PM collection system is designed to achieve a complete collection of the PM in the flue gas at point A. The total PM is dominantly collected in the cyclone (~90%) while the PM_{10} collected in the DLPI contributes to only ~10% of the total PM.

Figure 3 presents the similar data on the yields and mass concentrations of $PM_{1.0}$ and the particulate matter with an aerodynamic diameter between 1.0 and 10.0 μm ($PM_{1.0-10}$) and PM_{10}. Three key observations can be made from the data in Figure 3. First, regardless of the biomass feeding rate (0.1 or 0.3 g/min), the yield and mass concentration of PM_{10} actually increases with increasing sampling temperature from 25 to 105 °C and then levels off with a further increase to 115 °C. It seems that unless the sampling temperature is close to the flue gas temperature (115 °C), some of PM_{10} was collected by the sampling system before entering into the DLPI. Second, it is interesting to see that the sampling temperature has little effect on the yield and mass concentration of $PM_{1.0}$. Therefore, although the sampling temperature does influence the yield and mass concentration of PM_{10}, such influence is mainly on $PM_{1.0-10}$, as is clearly illustrated in Figure 3. Third, at the same sampling temperatures < 105 °C (such as 25 or 40 °C), increasing biomass feeding rate from 0.1 to 0.3 g/min has little effect on the yield of PM_{10}. However, increasing biomass feeding rate does lead to an appreciable reduction in the yield of $PM_{1.0}$, and interestingly, such a reduction is accompanied with an increase in the yield of $PM_{1.0-10}$. Therefore, the data in Figure 3 clearly suggest that the sampling temperature significantly influence the measured yield and mass concentration of PM_{10} in the flue gas, and such influence is also dependent on the source PM_{10}-containing flue gas.

3.2. Mass-Based Particle Size Distribution of PM_{10}. Further efforts were then made to investigate the mass-based particle size distribution (PSD) of PM_{10} collected at various sampling temperatures (see Figure 4). It can be seen clearly that the PSD of PM_{10} has a bimodal size distribution, i.e., a fine and a coarse mode. For example, at a biomass feeding

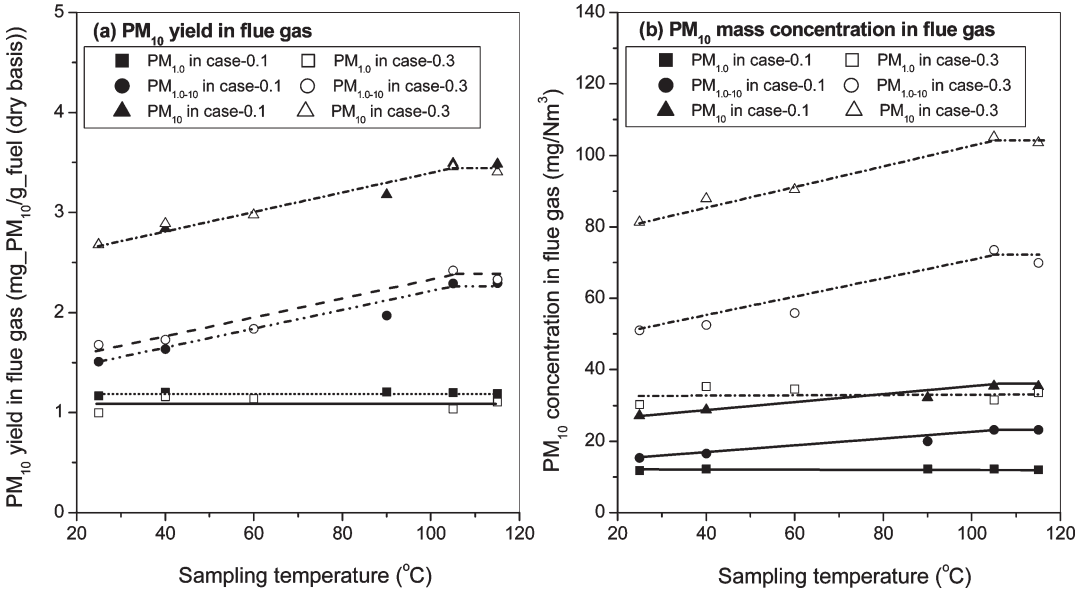

Figure 3. Emission characteristics of PM_{10} at various sampling temperatures: (a) PM_{10} yield in flue gas and (b) PM_{10} mass concentration in flue gas.

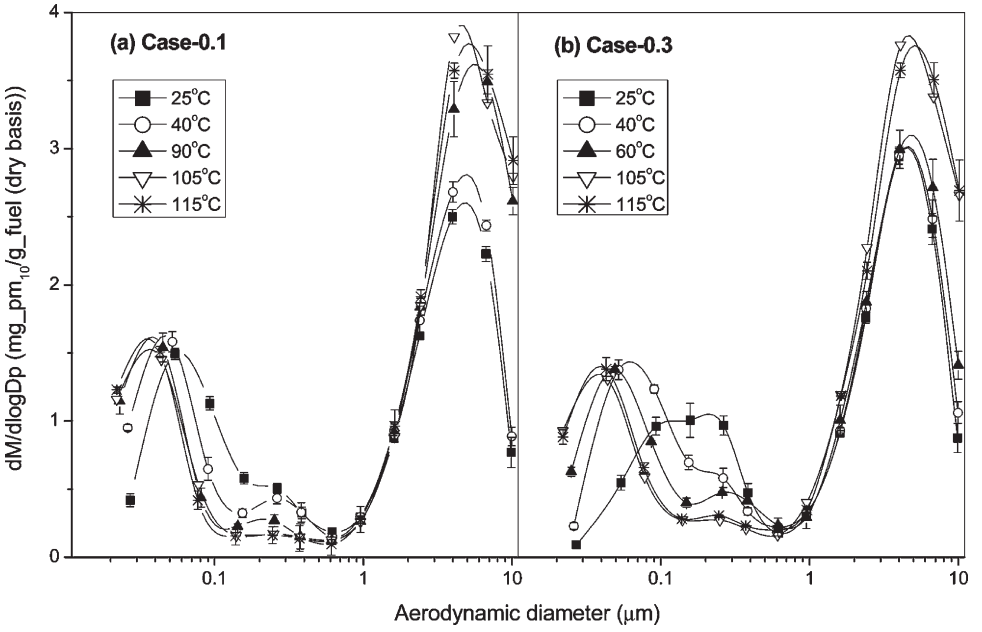

Figure 4. Mass-based particle size distribution of particulate matter collected by DLPI at different sampling temperatures: (a) Case-0.1 and (b) Case-0.3. Graphs are normalized to the total mass of bark sample (dry basis) fed into the drop-tube reactor in each experiment.

rate of 0.1 g/min, the fine mode is located between 0.03 and 0.1 μm with a mode diameter of ~0.05 μm while the coarse mode is located between 2.37 and 6.64 μm with a mode diameter of ~3.97 μm. A bimodal PSD of $PM_{10}$was reported in previous studies,[29,30]although the mode diameters were different possibly due to the differences in the fuels, experimental rigs, sampling systems, and sampling conditions used in the experiments.

However, the most important results in Figure 4 are the fact that the PSD of PM_{10} is significantly influenced by the sampling temperature. Although having little effect on the yield of $PM_{1.0}$ (see Figure 3), increasing sampling temperature shifts the PSD of $PM_{1.0}$ to smaller particle size. For $PM_{1.0-10}$, sampling temperature does not seem to influence the shape of the PSD curves. Rather, the mount of $PM_{1.0-10}$ collected increases as the sampling temperature increases from 25 to 105 °C and levels off from 105 to 115 °C, consistent with the data on PM_{10} yield in Figure 3. Clearly, the data in Figures 3 and 4 show that the influence of sampling temperature is distinctly different for $PM_{1.0}$ and $PM_{1.0-10}$, suggesting that there are likely different fundamental mechanisms governing the influence of sampling temperature on the collection and properties of $PM_{1.0}$ and $PM_{1.0-10}$. These aspects are discussed in the following sections.

3.3. Effect of Sampling Temperature on the Collection and Properties of $PM_{1.0}$ and $PM_{1.0-10}$. Figures 3 and 4 indicate

(29) Lind, T. T.; Valmari, E.; Kauppinen, K.; Nilsson, K.; Sfiris, G.; Maenhaut, W. *Proc. Combust. Inst.* **2000**, *28*, 2287–2295.
(30) Lind, T.; Kauppinen, E. I.; Hokkinen, J.; Jokiniemi, J. K.; Orjala, M.; Aurela, M.; Hillamo, R. *Energy Fuels* **2005**, *20*, 61–68.

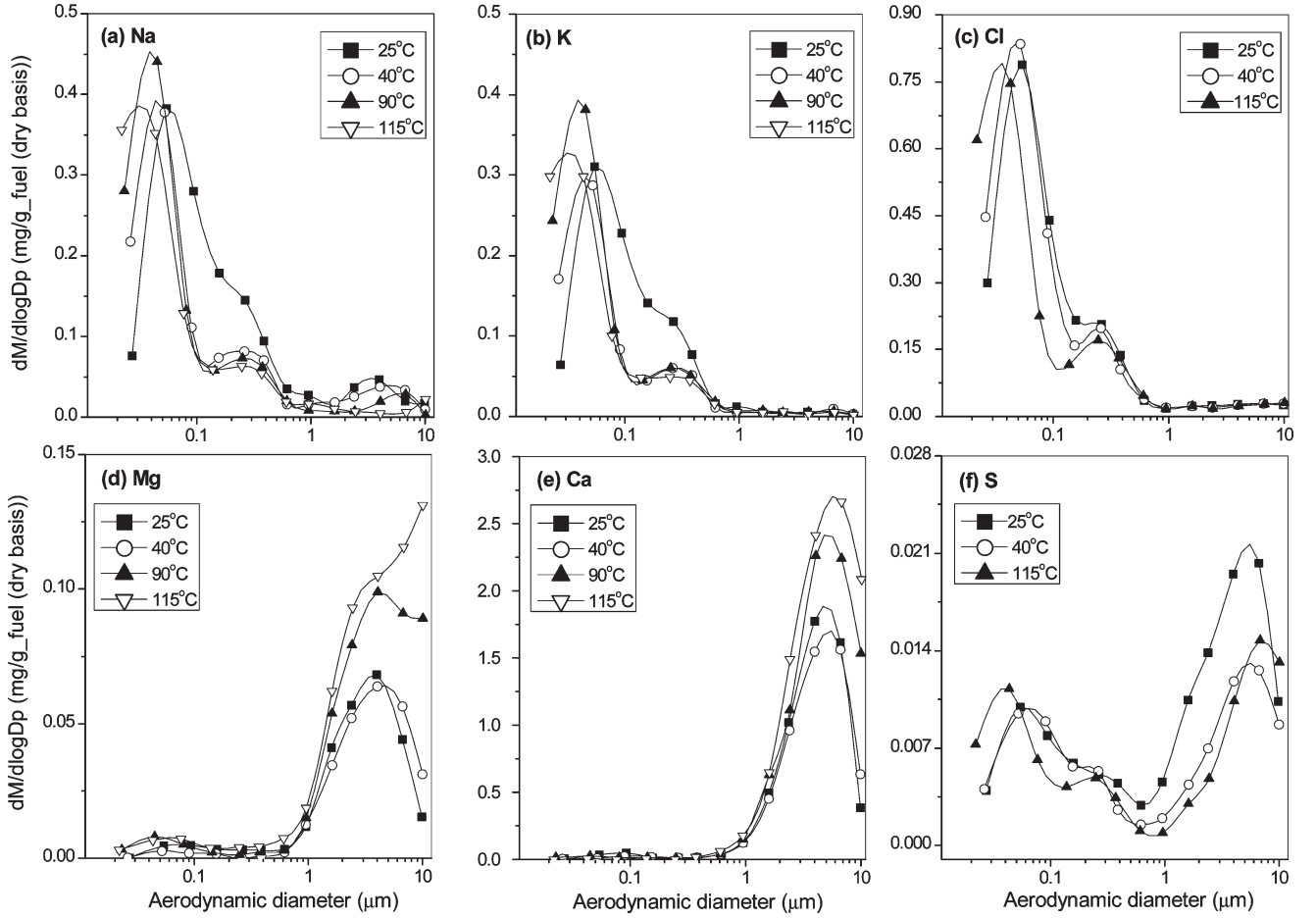

Figure 5. Elemental mass size distribution at different sampling temperatures in Case-0.1: (a) Na, (b) K, (c) Cl, (d) Mg, (e) Ca, and (f) S. Graphs are normalized to the total mass of bark sample (dry basis) fed into the drop-tube reactor in each experiment.

that the yield and PSD of $PM_{1.0}$ remain unchanged as the sampling temperature decreases from 115 to 105 °C. A further decrease in the sampling temperature leads to a decrease in the mass of PM with a size range from 0.03 to 0.05 μm, coupled with an increase in the mass of PM with a size range from 0.1 to 0.61 μm. While such a decrease is progressive, it becomes drastic as the sampling temperature decreased from a "turning point" temperature to 25 °C. The PSD of $PM_{1.0}$ is drastically influenced by the sampling temperature when it is below the "turning point" temperature. Such a "turning point" temperature is also dependent on the sampling source of the flue gas. For example, the "turning point" temperature increases from ~40 to ~60 °C, as the biomass feeding rate increases from 0.1 to 0.3 g/min. With respect to $PM_{1.0-10}$, the amount of PM with a size range from 2.37 to 10 μm increases significantly as the sampling temperature increases from 25 to 105 °C and remains unchanged as the sampling temperature further increases to 105 °C (see Figures 3 and 4).

Figure 5 (for Case-0.1) shows the elemental mass size distribution of Na, K, Mg, Ca, Cl, and S. It is shown that Na, K, Mg, Ca, and Cl all have a unimodal distribution. While Na, K, and Cl is dominantly contained in $PM_{1.0}$ in a single mode with a mode diameter around 0.05 μm, Mg and Ca are concentrated in $PM_{1.0-10}$ in a single mode with a mode diameter around 3.97 μm. The unimodal distribution of Na, K, and Cl in $PM_{1.0}$ is known to be the result of either homogeneous nucleation or heterogeneous condensation on small particles.[29,31−34] The unimodal distribution of Mg and Ca suggests that the $PM_{1.0-10}$ are likely produced from refractory elements (Mg and Ca) in the burning char particles.[29,31−33] However, S shows a clear biomodal distribution as shown in Figure 5f, with a fine mode around 0.05 μm and a coarse mode around 3.97 μm. The S in $PM_{1.0}$ mainly exists as the sulfates of alkali metals,[35] formed via either homogeneous[36−38] and/or heterogeneous[39−41] mechanisms. The S in $PM_{1.0-10}$ may be formed via the reactions between S and Ca,[42] condensation of alkali sulfates on the surface of

(31) Christensen, K. A. The formation of submicron particles form the combustion of straw. PhD dissertation. Technical University of Denmark, Lyngby, Denmark, 1995.
(32) Johansson, L. S.; Tullin, C.; Leckner, B.; Sjövall, P. *Biomass Bioenergy* **2003**, *25*, 435–446.
(33) Pagels, J. M.; Strand, J. R. *J. Aerosol Sci.* **2003**, *34*, 1043–1059.
(34) Hinds, W. *Aerosol Technology: Properties, Behavior, and Measurement of Airborne Particles*, 2 ed.; Wiley-Interscience: New York, 1999.
(35) Hindiyarti, L.; Frandsen, F.; Livbjerg, H.; Glarborg, P.; Marshall, P. *Fuel* **2008**, *87*, 1591–1600.
(36) Hanby, V. I. *J. Eng. Power* **1974**, *96*, 129–133.
(37) Kohl, F. J.; Santoro, G. J.; Stearns, C. A.; Rosner, D. E. *J. Electrochem. Soc.* **1979**, *126*, 1054–1061.
(38) Fielder, W. L.; Stearns, C. A.; Kohl, F. J. *J. Electrochem. Soc.* **1984**, *131*, 2414–2417.
(39) Steinberg, M.; Schofield, K. *Prog. Energ. Combust.* **1990**, *16*, 311–317.
(40) Steinberg, M.; Schofield, K. *Proc. Combust. Inst.* **1996**, *26*, 1835–1843.
(41) Srinivasachar, S.; Helble, J. J.; Ham, D. O.; Domazetis, G. *Prog. Energ. Combust.* **1990**, *16*, 303–309.
(42) Baxter, L. L.; Miles, T. R.; Dayton, D.; Bryers, R. W.; Oden, L. L. *Fuel Process. Technol.* **1998**, *54*, 47–78.

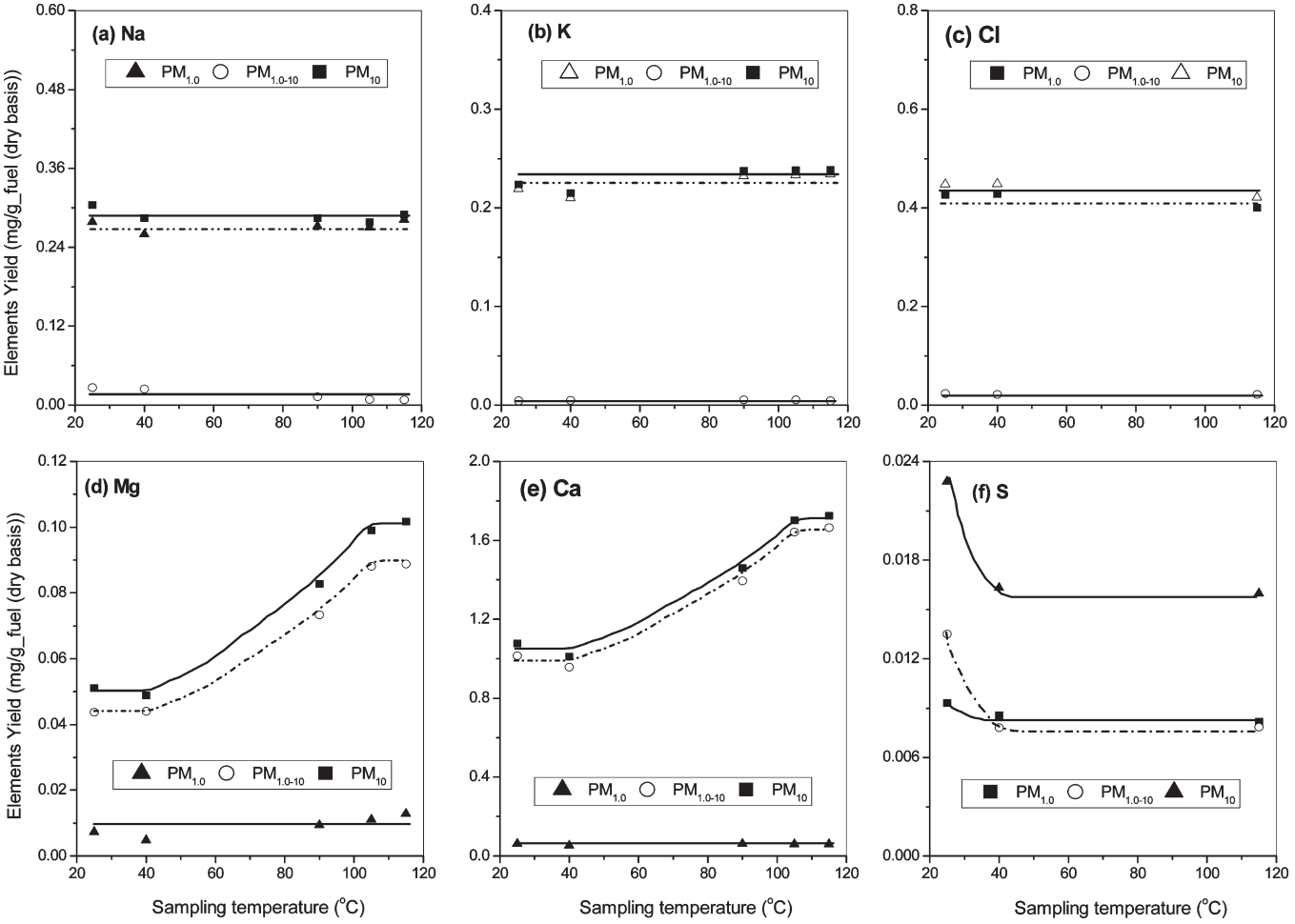

Figure 6. Summary of element yields at different sampling temperatures in Case-0.1: (a) Na, (b) K, (c) Cl, (d) Mg, (e) Ca, and (f) S. Graphs are normalized to the total mass of bark sample (dry basis) fed into the drop-tube reactor in each experiment.

coarse particles,[8] coagulation of S-rich small particles on the coarse particles, and/or condensation of SO_3 during sampling process.

Figure 5 also clearly shows, that for $PM_{1.0}$, decreasing sampling temperature results in a progressive decrease in the mass of Na, K, and Cl in the size range of 0.03−0.05 μm, and an increase in the mass of these elements in the size range of 0.1−0.61 μm. The changes in the Na, K, and Cl distribution curves as a function of sampling temperature also exhibit a "turning point" temperature of 40 °C, consistent with that of the PSD curves (see Figure 4a). However, the mass of Mg and Ca in $PM_{1.0-10}$ increases as the sampling temperature increases from 25 to 105 °C and remains unchanged from 105 to 115 °C (see Figure 6d,e). With respect to S (see Figure 5f), as the sampling temperature decreases, the S mass also shifts to a larger size in $PM_{1.0}$. The S distribution curve at the "turning point" temperature (40 °C) has a similar trend with that of 25 °C in the size range of 0.03−0.38 μm, but there is a considerable increase in the mass of S in the size range of 0.38−6.64 μm when the sampling temperature decreases to 25 °C. Furthermore, the S distribution curve in $PM_{1.0-10}$ at the turning point temperature (40 °C) is similar with that of 115 °C, while S in the size range of 0.942−6.64 μm increases significantly as the sampling temperature decreases to 25 °C. The results suggest that S has condensed from the stage with a 50% aerodynamic cutoff diameter (D50) of ~0.38 μm at sampling temperatures blow the "turning point" temperature (40 °C).

Therefore, the data in Figures 3−5 suggest that the presence of the "turning point" temperature in the mass and elemental mass PSD curves is related to the condensation of sulfur. On the basis of the estimated flue gas compositions, the dew point temperature of SO_3 and HCl in the flue gas can be estimated using the following well-known equations:[43,44]

$$T_{d,SO_3} = 1000/\{2.276 - 0.0294\ln(P_{H_2O}) - 0.0858\ln(P_{SO_3}) + 0.0062\ln(P_{H_2O}) \times \ln(P_{SO_3})\} \quad (1)$$

$$T_{d,HCl} = 1000/\{3.7368 - 0.1591\ln(P_{H_2O}) - 0.0326\ln(P_{HCl}) + 0.00269\ln(P_{H_2O}) \times \ln(P_{HCl})\} \quad (2)$$

where T_{d,SO_3} and $T_{d,HCl}$ are the dew point temperature of SO_3 and HCl (K) and P_{H_2O}, P_{SO_3}, and P_{HCl} are the partial pressure of H_2O, SO_3, and HCl in the flue gas (mmHg). It should be noted that the acid dew point temperature decreases from top stage to bottom stage of the DLPI because the flue gas pressure decreases progressively from 1013.3 mbar in top stage to 100 mbar in bottom stage of DLPI, and the partial pressure of acid gas decreases in the downstream of the DLPI as the result of progressive condensation. The SO_3 and HCl dew point temperatures at the top stage of DLPI

(43) Verhoff, F. H.; Branchero, J. *Chem. Eng. Prog.* **1974**, *70*, 71.
(44) Kiang, Y. H. *Chem. Eng.-New York* **1981**, *88*, 127.

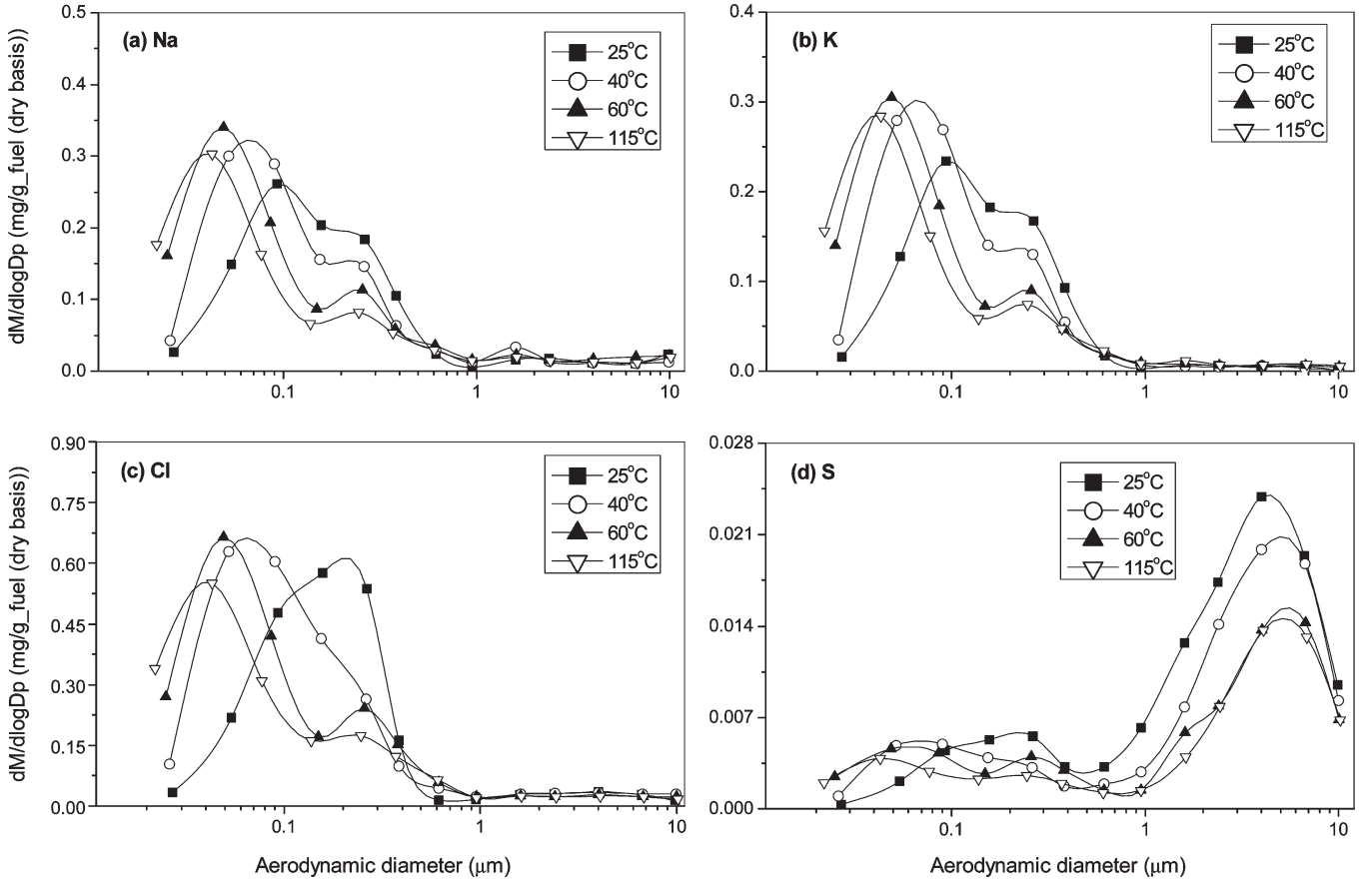

Figure 7. Elemental mass size distribution at different sampling temperatures in Case-0.3: (a) Na, (b) K, (c) Cl, and (d) S. Graphs are normalized to the total mass of bark sample (dry basis) fed into the drop-tube reactor in each experiment.

are estimated to be 45 and 4 °C, respectively. Indeed, the "turning point" temperature of PSD curves correlates well with the calculated SO_3 dew point temperature, as HCl is not likely to condense in the collection system even at the lowest sample temperature (25 °C). Additionally, the temperature of flue gas (115 °C) in this study is low enough for the complete nucleation and condensation of alkali vapors;[45] complete combustion of biomass in the DTF system was also achieved so that little organic species vapors would be present in the flue gas. Therefore, SO_3 condensation is a key mechanism governing the effect of sampling temperature on the properties of collected $PM_{1.0}$.

Furthermore, as shown in Figure 5f, the amount of S condensed in $PM_{1.0}$ and $PM_{1.0-10}$ is very small in comparison to the $PM_{1.0}$ and $PM_{1.0-10}$ yield (see Figure 3); hence, it contributes little to the total mass of $PM_{1.0}$ and $PM_{1.0-10}$. However, the data in Figure 6f show that the amount of S has a considerable increase in $PM_{1.0}$ and a significant increase in $PM_{1.0-10}$ at the sampling temperature below the "turning point" temperature (40 °C), and S condenses mainly on coarse particles due to the SO_3 dew point temperature being lower in the downstream stages of the DLPI.

To further identify the relationship between the "turning point" temperature of PSD curves and the calculated SO_3 dew point temperature, the biomass feeding rate was increased to 0.3 g/min. In this case, the dew point temperatures of SO_3 and HCl in flue gas at the top stage of the DLPI are

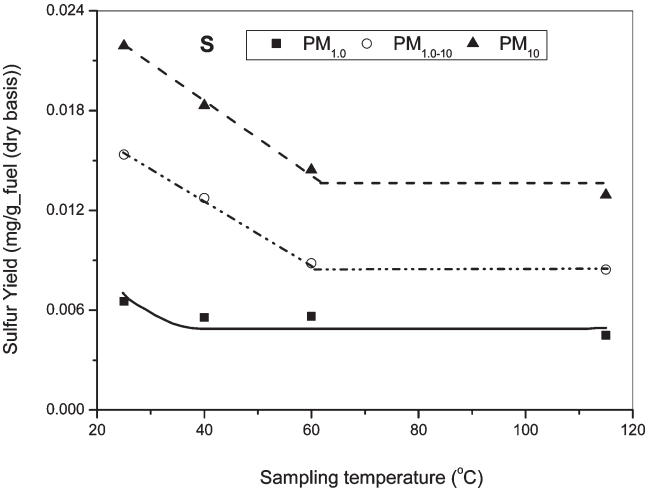

Figure 8. Sulfur yields at different sampling temperatures in Case-0.3. Graphs are normalized to the total mass of bark sample (dry basis) fed into the drop-tube reactor in each experiment.

estimated to be 65 and 15 °C, respectively, due to the higher acid gas concentration compared with that at 0.1 g/min; note that HCl is still not likely to condense even at the lowest sampling temperature (25 °C). As shown in Figures 7 and 8, it is clear that SO_3 starts to condense at the sampling temperature below 60 °C, which is in good agreement with the calculated SO_3 dew point temperature. Furthermore, the "turning point" temperature of 60 °C observed from PSD curves (see Figure 4b) and elemental mass size distribution

(45) Boman, C.; Nordin, A.; Boström, D.; Öhman, M. *Energy Fuels* **2004**, *18*, 338–348.

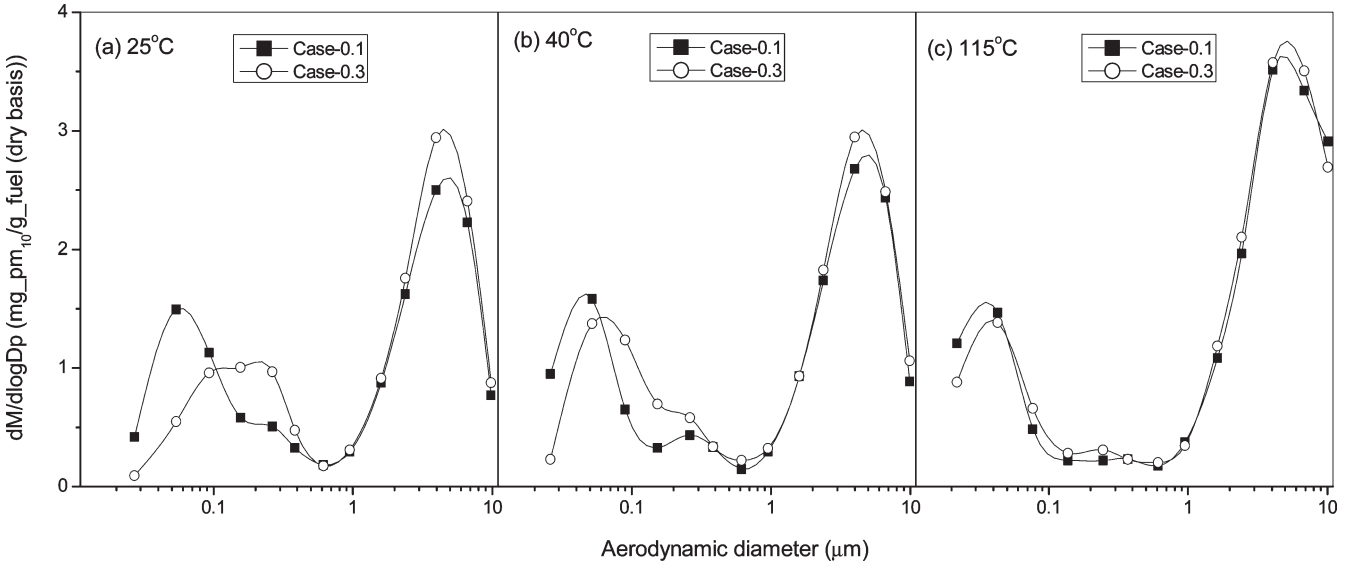

Figure 9. Effect of biomass feeding rate on PSD curves at different sampling temperatures: (a) 25 °C, (b) 40 °C, and (c) 115 °C.

curves (see Figure 7) indeed correlates well with the calculated SO_3 dew point temperature.

3.4. Possible Mechanisms Responsible for the Effect of Sampling Temperature on the Collection and Properties of PM_{10}. Three mechanisms may be responsible for the effect of sampling temperature on the collection and properties of PM_{10}, i.e., thermophoresis deposition, coagulation of fine particulate matter, and gravitational settling deposition. Thermophoresis, mainly influencing the transport loss of submicrometer particles,[46] is a result of a temperature gradient in the surrounding gas, resulting in a particle being drawn into the direction of decreasing temperature.[34] Particle coagulation is a process where fine particles collide with one another due to their relative motion and adhere to form larger particles, as the result of Brownian motion and/or external forces.[34] Gravitational settling deposition takes place due to the gravity and has more of an effect on coarse particles than fine particles.[34]

Relevant to this study, thermophoresis deposition is not expected to be important due to the small temperature differences. In fact, the nearly constant amount of $PM_{1.0}$ under different sampling temperature (see Figure 3) already indicates that the effect of thermophoresis deposition is negligible under the experimental conditions.

Coagulation of fine particles appears to be the key mechanism, as it does not change the total $PM_{1.0}$ mass but only shifts the $PM_{1.0}$ PSD. The coagulation process is also influenced by temperature.[47] As flue gas temperature decreases, the flue gas velocity decreases, resulting in enhanced relative motions among the particulate particles, and consequently, the coagulation process is enhanced. This is indeed the case as seen in Figure 4 which shows a progressive growth of particle size in $PM_{1.0}$, as sampling temperature decreases. Coagulation of fine particles is also accelerated by the sulfuric acid droplets at the sampling temperature below "turning point" temperature (also SO_3 dew point temperature as discussed), although SO_3 condensation contributes little to the PM_{10} yield. The accelerated coagulation causes a significant shift of particle mass to a larger size in $PM_{1.0}$ (see Figure 4). As discussed, the "turning point" temperature in PSD curves correlates well to the calculated SO_3 dew point. Therefore, SO_3 condensation plays an important role in the coagulation process and, therefore, the effect of sampling temperature on the properties of collected $PM_{1.0}$.

Further elemental analysis shows that the total amounts of Na, K, and Cl in $PM_{1.0}$ are nearly constant at all the sampling temperatures (see Figure 6). The shifts of size distribution curves of these elements at different sampling temperatures (see Figure 5) is, therefore, most likely due to the coagulation of Na-, K-, and Cl-containing particles. So is the mass shift of S in a size range of 0.03−0.38 μm (see Figure 5f). Therefore, all the data suggest that coagulation of fine particulate matter is the key mechanism responsible for the shifts of PSD and elemental mass size distribution curves of $PM_{1.0}$.

The coagulation process seems to also be influenced by the concentration of particulate matter in flue gas. Figure 9 is based on the data in Figure 4 and clearly shows that, as the biomass feeding rate increases from 0.1 to 0.3 g/min (i.e., Case-0.1 and Case-0.3, corresponding to an increase in the PM concentration in the flue gas by 3 times), the particle mass shifts to a larger size in $PM_{1.0}$ when the particle number concentration increases at the sampling temperature of 25 and 40 °C. However, such an effect diminishes at a sampling temperature close to the flue gas temperature (115 °C), suggesting that a sampling temperature close to the flue gas temperature is required in order to suppress particle coagulation. Although the PM_{10} yield is nearly constant for both Case-0.1 and Case-0.3, the $PM_{1.0}$ yield in Case-0.3 is slightly lower and the $PM_{1.0-10}$ yield is slightly higher compared to those in Case-0.1 (see Figure 3), suggesting that some fine particles in $PM_{1.0}$ have coagulated with coarse particles in $PM_{1.0-10}$ due to the higher PM concentration in Case-0.3.

Gravitational settling deposition has more of an effect on coarse particles.[34] In fact, as the sampling temperature decreases, the particle loss caused by gravitational settling deposition increases as a result of decreasing flue gas velocity, resulting in part of an increasing loss of PM before the PM_{10}-containing flue gas enters into the DLPI. This is indeed the case as both the yield of $PM_{1.0-10}$ and the mass of Mg and

(46) Mackowski, D. W.; Tassopoulos, M.; Rosner, D. E. *Aerosol Sci. Technol.* **1994**, *20*, 83–99.
(47) Alonso, M.; Alguacil, F. J.; Martin, M. I.; Kousaka, Y.; Nomura, T. *J. Aerosol Sci.* **1999**, *30*, 1191–1199.

Ca in $PM_{1.0-10}$ decreases with decreasing sampling temperature (see Figures 3−6). The similar trend of PSD curves at the sampling temperature of 105 and 115 °C (see Figure 4) further suggests that in order to eliminate the influence of gravitational settling deposition on the collection of $PM_{1.0-10}$, the sampling temperature must be close to or the same as the flue gas temperature (115 °C).

4. Conclusions

The experimental data in this study clearly demonstrate the significant effects of sampling temperature on the collection of PM_{10} and its properties. Coagulation of fine particles appears to be the key mechanism responsible for the shift of $PM_{1.0}$ mass to larger size as the sampling temperature decreases, although the total yield of $PM_{1.0}$ remains unchanged. The chemical composition of $PM_{1.0}$ is dominantly Na, K, and Cl, and the mass distribution of these elements also shifts to a larger size in $PM_{1.0}$ as the sampling temperature decreases, as a result of the coagulation of Na-, K-, and Cl-containing fine particles. However, the $PM_{1.0-10}$ dominantly contains Mg and Ca; the mass of $PM_{1.0-10}$ and the mass of Mg and Ca in $PM_{1.0-10}$ increases with increasing sampling temperature and levels off at a sampling temperature close to the flue gas temperature (115 °C). The reduction in the collection of Mg- and Ca-containing coarse particles in $PM_{1.0-10}$ as the sampling temperature decreases appears to be mainly due to gravitational settling deposition. The "turning point" temperature of PSD and elemental mass size distribution curves seems to correlate well with the SO_3 dew point of the flue gas. Therefore, to ensure the proper collection of PM_{10}, the sampling temperature should be above the flue gas acid dew point temperature to prevent acid gas condensation and, furthermore, be kept at a temperature close to or the same as the flue gas temperature.

Acknowledgment. This study is sponsored by Australia's Department of Innovation, Industry, Science, and Research through the Australia-China Special Fund for S&T Cooperation (CH070008). X.G. is grateful to the EIPRS scholarship from Australia's Department of Education, Employment and Workplace Relations and the CUPS scholarship from Curtin University for his PhD study.